ISSN 0029 - 3865

CBPF-NF-013/85

MAGNETIC PROPERTIES OF $Ce(Fe_{1-x}Al_x)$ FOR $x \leq 0.20$

RUNNING TITLE: MAGNETIC PROPERTIES OF $Ce(Fe_{1-x}Al_x)_2$

by

D.F. Franceschini and S.F. da Cunha

Centro Brasileiro de Pesquisas Físicas - CBPF/CNPq
Rua Dr. Xavier Sigaud, 150
22290 - Rio de Janeiro, RJ - Brasil

ABSTRACT

Magnetization measurements of the system $Ce(Fe_{1-x}Al_x)_2$ for $x \leq 0.20$ show that the substitution of Fe by Al in $CeFe_2$ has not a simple dilution effect. Together with a accentuated decrease in the iron mean magnetic moment and in Curie temperatures was observed, above a certain concentration, a transition from ferromagnetism to a canted spin phase upon decreasing temperature. For the higher concentration range the system exhibits magnetic freezing effects. A preliminary magnetic phase diagram was proposed.

Key-words: Magnetization of Laves phase; $Ce(FeAl)_2$ compounds; Canted spin phase; Magnetic phase diagram.

1 - INTRODUCTION

Pseudo-binary systems $R(Fe_{1-x}Al_x)_2$ (R = Rare Earth metal, Y, Zr or Sc) have been investigated by several authors [1,2,3]. The end compounds RFe_2 and RAl_2 in almost all cases crystalize in the Cubic Laves Phase structure $MgCu_2$ type. In the pseudo-binary systems the structure for the intermediate concentration range belongs to the $MgZn_2$ hexagonal type. When R is magnetic, the effect of iron substitution on the magnetic behavior is to reduce the strength of the magnetic interactions, which induces the decrease of the magnetic transition temperatures T_c and the iron mean magnetic moments μ_{Fe}. When R is non-magnetic such effect is much more intense, giving rise to the lack of long range magnetic order at a critical concentration x_c. Thus, an interesting feature of those systems is to investigate the onset of magnetism, recently reviewed by Hilscher [2].

The transition from ferromagnetic order to a non-magnetic one in $R(Fe_{1-x}Al_x)_2$ when R is non-magnetic, occurs in two different ways. For Zr[2] and Sc[3] systems, iron substitution induces only magnetic dilution, leading to a decrease of both T_c and μ_{Fe} until vanishing at x_c. For $Y(Fe_{1-x}Al_x)_2$ system [2], the transition from magnetically ordered to disordered state is intermediated by a concentration range which shows mictomagnetic or spin glass behaviour. This kind of behaviour gives rise to a magnetic phase diagram analogous to that observed in qualitatively

different systems like AuFe or $(Eu_{1-x}Sr_x)S$. This feature is an indication that there is not only magnetic dilution, but an exchange competition is also taking place.

The ferromagnetic compound $CeFe_2$ is a special case among the AFe_2 compounds (A = Y, Zr, Sc, Lu). Its Curie temperature T_c and the iron mean magnetic moment μ_{Fe} (T_c = 230K, μ_{Fe} = 1.24μ_B) are somewhat smaller than those of other similar compounds. This difference has been attributed to some transfer of the Ce 4f electron to the conduction band [4], and would make $CeFe_2$ more sensitive upon iron substitution. Concerning $Ce(Fe,Al)_2$ only a few preliminary studies are reported. Dwight et al. [5] have studied the crystal structure of several $R(Fe,Al)_2$ but paid little attention to the case of Ce. In their work there is only a comment about the small solubility range at the iron-rich side. Da Cunha et al. [6] and Takeuchi et al. [7] have respectively studied the behaviour of the magnetization and electrical resistivity in $Ce(Fe_{0.8}Al_{0.2})_2$. Those works report a well stabilished spin glass behaviour at low temperature and at a higher temperature, a sharp maximum in the magnetization versus temperature curve, which was not completely explained.

The aim of this work is to extend the study of the magnetic properties of the pseudobinary compounds $Ce(Fe_{1-x}Al_x)_2$ trying to elucidate some unusual features observed in [6] and [7]. Here we report and discuss the temperature and field dependences of the magnetization for some concentrations $0 \leq x \leq 0.20$. Electrical resistivity measurements on the same samples will appear in [8].

2 - EXPERIMENTAL

The samples were prepared by melting stoichiometric amounts of the components in an arc furnace under a purified argon atmosphere. The nominal purity of the starting elements are of 99.99% for Ce (Rare Earth Products Ltd.), 99.99% for Fe and 99.995%, for Al (Johnson Matthey Inc.).

The samples are remelted three or four times and annealed for a week at 700ºC in an argon atmosphere. After, they were quenched in liquid nitrogen. The crystal structure and lattice parameter were determined by X-ray diffraction analysis on powdered samples. The X-ray patterns for the $x \leq 0.10$ samples exhibit a single phase characteristic of the $MgCu_2$ type structure. For $x \geq 0.125$ the X-ray patterns show together with $MgCu_2$ lines, extra lines of foreign phases (CeAl and other unidentified lines). Different stoichiometries and thermal treatments did not eliminate those foreign phases. The lattice parameters a_o were derived by least square analysis using Nelson-Riley's extrapolation. The concentration dependence of the lattice parameter is shown in fig 1, where we can see a linear dependence for $x \leq 0.10$ and a rought constant value for $x \geq 0.125$. This kind of behaviour —together with the presen - ce of extra lines in the X-ray patterns —suggests that the solubility limit to form the pure $MgCu_2$ type structure for $Ce(Fe_{1-x}Al_x)_2$ may be placed near $x = 0.125$. The comparison between the linear portion of the a_o vs x plot and the Vegard's law line for the $CeFe_2$ -$CeAl_2$ system (dot-dashed line)suggests that the Ce ions must

be in the same valence state of the $CeFe_2$ compound up to the solubility limit as explained in [8].

Magnetization was measured using a P.A.R. vibrating sample magnetometer operating at a frequence of 80 Hz and over a temperature range of 3-300K in magnetic fields up to 13 kOe. Some magnetization measurements were made using a superconducting coil with fields up to 80 kOe or an extraction magnetometer (SNCI-GRENOBLE) with fields up to 150 kOe. Temperature sensors of carbon, chromel-Au-Fe and Cu-constantan thermocouples were used. The absolute accuracy of the temperature determination was about $\pm$ 1 K.

3 - EXPERIMENTAL RESULTS AND DISCUSSION FOR $x \leq 0,10$

3.1 - Results

The temperature dependence of the magnetization for $x \leq 0.07$ in a magnetic field of 1kOe is shown in fig. 2 and of 10 kOe in fig 3. The curves were obtained after the samples had been cooled in zero field from room temperature and measured increasing the temperature and then remeasured during the cooling process.

Firstly we can observe for $0.0 \leq x \leq 0.035$ that at least in some temperature range a ferromagnetic behaviour is present. The curve obtained for $x = 0.02$ under an applied field of 1kOe shows for $T < 50K$, a small but continuous decrease in the magnetization upon decreasing temperature acompained by thermomagnetic irreversible effects; under 10kOe such effects are absent and the curve is characteristic of a ferromagnetic behaviour.

For $x = 0.035$ the decrease in magnetization below about 70K and the thermomagnetic irreversible effects are more accentuated as compared to $x = 0.02$ even for a 10 kOe applied field and the temperature for which these effects do appear depends on the applied field. In the concentration $x = 0.07$ the decrease in magnetization with decreasing temperature takes place at a higher temperature and a maximum appears at 145K; we have a monotonic behaviour at low temperatures. The $x = 0.10$ concentration shows a similar behaviour to $x = 0.07$.

In fig 4 high field magnetization curves up to 80 kOe at 4.2K for $0.00 \leq x \leq 0.07$ are shown.

For $x = 0.0$ and 0.02 the curves are characteristic of ferromagnetic behaviour, showing knee and saturation. For $x = 0,035$ the lower field portion of the curve exhibit a marked curvature, showing tendency to saturation; the higher field portion however shows a magnetization step at a critical field of about 35 kOe, above which the magnetization begins to saturate. This curve shows also the development of a large histeresis loop which is, together with the magnetization step, characteristic of metamagnetism. For $x = 0.07$ the behaviour seems to be reminiscent of the $x = 0.035$ one, although with a much higher critical field ($H_c > 80$ kOe) and a negligeable curvature in the lower field portion of the magnetization curve.

Hysteresis loops for $x \leq 0.035$ at low temperature for fields between - 13 and 13 kOe were observed. For $x = 0,0$ and $x = 0.02$ very narrow hysteresis loops were obtained. For $x = 0.035$ (fig. 5), we have different behaviour if the sample is

cooled in zero field or in 13 kOe although the two loops are centred at the origin.

Isothermal magnetization versus field curves up to 13 kOe were obtained for various temperatures. For x = 0.02 (fig.6), we observe at low temperatures a dependence of the initial slope with temperature. For x = 0.035 (fig.7), in the temperature range below 70K of decreasing magnetization, we have hysteresis loops with no magnetic remanence for H = 0 and for T > 70K typical ferromagnetic behaviour was observed (fig.8). For x = 0.07 (fig.9) the observed upturns of the M_g vs H curves disappear at temperatures near the maximum of the M_g vs T curves.

3.2 - Discussion

$CeFe_2$ is a known ferromagnetic intermetallic with Curie temperature T_c = 230K. For x = 0.02 the low temperature decrease in the M_g vs T curve is related to the variation of the inicial slope of the M_g vs H curves for T < 50K. For T > 50K a normal ferromagnetic behaviour is observed; the spontaneous magnetization at 4.2K is consistent with that of $CeFe_2$, the low temperature anomalies been explained in terms of the difficult motion of domain wall. Also, the coercive field for x = 0.02 is larger than for x = 0.0.

The sharp decrease in the isofield magnetization curves for x = 0.035 reveals a substantial reduction of the spontaneous magnetization, thus characterizing a change in the type of the magnetic structure. The observed thermo-remanent effects could

be ascribed to a ferromagnetic-spin glass like transition, similar to that observed in $Y(Fe,Al)_2$ [9]. However, the low field histeresis loops obtained at 4.2K (fig.5) do not confirm this hypotesis since the loops are centred at the origin. So, the iron magnetic moments must be ordered in a non collinear manner, i.e. the magnetization has a ferromagnetic plus an antiferromagnetic component say a canted spin structure. The high field magnetization curve at 4.2K (fig.4) and the low field isothermal curves (fig.7) do corroborate this point. These results show a turning point in the magnetization curves at a critical field H_c, characteristic of a magnetic transition to a more ordered state along the field. We can see that critical fields H_c decrease with increasing temperature, until vanishing. At the vanishing point of H_c, the isothermal magnetization curves show clearly a ferromagnetic behaviour.

The results for x = 0.07 indicate a very similar behaviour to that of x = 0.035. Appart from the higher critical fields H_c and much smaller difference between the transition temperatures of the canted -ferro and ferro-para transitions, the magnetization curves can be explained in the same way. The high field magnetization curve at 4.2K looks like those obtained for x = 0.035 with low field and is showed in fig.7. The M_g vs H curves for T >77K (fig 9a) show a temperature dependent critical field H_c, which vanishes at a temperature very close to the peak. In fig.9b we can see that the magnitude of the magnetization is about the same order as the obtained for x = 0.02 and x=0.035 at temperatures near T_c. So, this result indicates a probable ferromagnetic ordering of iron magnetic moments. Fig.10

shows the date of figs.9a and 9b plotted as M_g vs T curves. These curves show an effect of the increasing applied field similar to that observed for x = 0.035.

The Curie temperature T_c and the iron mean magnetic moment μ_{Fe} were determined for all samples with $0,0 \leq x \leq 0.07$ and are listed in table 1. Curie temperatureswere determined from $(M_g)^2$ vs T plots of low field (150 Oe) magnetization data. An example is shown in the insert of fig.10. The iron moments μ_{Fe} were determined at 4,2K from magnetization data obtained for magnetic field of 80 kOe. The room temperature M_g vs H curves for this sample show however a small but not negligeable, magnetic impurity contribution. The magnetization due to these impurities was subtracted from the obtained extrapolation value at T = 4,2K. As in other systems, both magnetic moment and Curie temperatures decrease sharply upon increase of Al concentration as show in fig.11. Data for Y $(Fe_{1-x}Al_x)_2$ taken from [10] are plotted in the same figure for comparison.

4 - EXPERIMENTAL RESULTS AND DISCUSSION FOR x>0.10

4.1 - Results

The temperature and field dependences of the magnetization were measured in samples with composition $x \geq 0.125$. The M_g vs T curve for x = 0.15 measured with H = 1 kOe and zero field cooled is shown in figure 12 and is characteristic of the range $0.125 \leq x \leq 0.20$. At high temperatures we can observe a peak, the same behaviour as observed for x = 0.07. However, at low tempe-

ratures, a second peak appears at T_f for all the three compositions at temperatures which vary from 10K to 15K. To investigate the origin of the low temperature peak, as in [6] we have performed measurements after the samples had been cooled in zero field from high temperature to 3K, and then measured in monotonical increase of temperature up to about 30K with an applied field of 300 Oe. These curves presents irreversible effects for $T<T_f$ but reversibility occurs for $T>T_f$. Afterwards the magnetization has been measured in a field H = 300 Oe but now during the cooling process from 30K to 3K. Once the lowest temperature is achieved the magnetization is re-measured for increasing temperature. The variation is observed to be identical to that measured during cooling with a constant applied field of 300 Oe thus been reversible within the time scale of the experiment (a few minutes per experimental point). An example of these measurements is shown in figure 13. For 1 kOe applied fiels the same characteristic behaviour is observed but with a broader and lower intensity peak and with a slight shift of T_f.

In fig.14 we present typical isothermal magnetization versus field curves for fields up to 150 kOe. These curves show the same metamagnetic behaviour as that of x = 0.035, but with no indication of saturation.

4.2 - Discussion

As it was explained in section 2, the samples for $x \geq 0.125$ exhibit, besides of the cubic C15 structure, the presence of foreign phases like CeAl. This compound is antiferromagnetic with a Néel temperature of 10K [11,12]. Our expe-

rimental results for x≥0.125 at low temperatures, are typical of freezing phenomena characterised by different susceptibility behaviours as samples were cooled with or without field. Other results that corroborate this idea are the variation of the susceptibility with temperature for different valuesof frequency as we can see in figure 15, and also the displaced hysteresis loops at low temperature, figure 16.

The fact that the lattice parameter a_o and the residual resistivity ρ_o [8] becomes roughly constant in this concentration range suggest that possibly the $MgCu_2$ dilution limit of the $CeFe_2$ - $CeAl_2$ system for the iron rich side is attained.

The low temperature maximum of the magnetization observed in these samples cannot be atributed to tbe CeAl phase. Since there are other unidentified phases in that composition range, we by no means can be sure that the observed spin glass behaviour is intrinsic to the $MgCu_2$ $Ce(Fe_{1-x}Al_x)_2$ phase. So, more detailed work near the probable solubility limit must be done to elucidate this matter.

The high field magnetization data for x = 0.15 show characteristic featuresof magnetic behaviour at the canted spin temperature range. In fig. 14 we can see the strong variation of H_c and the width of the histeresis loop as the temperature changes. The higher critical field H_c = 110 kOe at 4.2K - as compared to that observed for x = 0.035, confirms the tendency insinuated in x = 0.07 composition.

5 - CONCLUSION

Magnetization measurements of the pseudobinary system $Ce(Fe_{1-x}Al_x)_2$ for $x \leq 0.20$ show that the substitution of Fe by Al in $CeFe_2$ has not a simple dilution effect. Together with the usual decreases in the iron mean magnetic moment μ_{Fe} and in the ferromagnetic Curie temperature T_c, we observe a transition from ferromagnetism to a non-collinear order, upon decreasing temperature, above a certain concentration. For the higher concentration range the system exhibits magnetic freezing effects. As in $Y(FeAl)_2$ or Fe-Al the disorder produced by the Al adition gives rise to a negative exchange competing with the positive, ferromagnetic one [13].

For $x<0,10$ ferromagnetic order is present in some temperature range and for $0.035 \leq x \leq 0.10$ changes in magnetic structure take place at low temperature with moment ordered probably in a non-collinear way. For $x = 0$ and 0.02 only ferromagnetic behaviour was observed. For $0.035 \leq x \leq 0.10$ the transition from a ferromagnetic to a non-collinear order was indicated by jumps in the M_g vs T curves. This low temperature magnetic phase exhibits metamagnetic behaviour, which was indicated by steps and large histeresis loops in the M_g vs H curves.

The electrical resistivity measured in the same samples $x \geq 0.10$ as a function of temperature [8] exhibits two minima, the low temperature one is expected to be related to a spin-glass state. The higher temperature minimum corresponds to the temperature at which $H_c = 0$ or to the jump in M_g vs T curves if

measurements have been made in zero field. In general, the shape of the M_g vs T curves may be explained in the following way. If the temperature T_o, where the critical field H_c equalizes the applied field in measurements of M_g vs T, is much lower than T_c (Curie temperature), ferromagnetic behaviour will dominate in some range of temperature as in x = 0.035. On the contrary, if $T_o \sim T_c$, the M_g vs T curves will exhibits a narrow peak as observed in x = 0.07. So the high temperature resistivity minimum [8] was found to be related to this transition and may be ascribed to an extra scattering mechanism introduced by the disorder in the magnetic structure. For $x \geq 0.125$ we observe a well characterized spin-glass behaviour at low temperature.

Finally, we propose a preliminary magnetic phase diagram for the iron rich side of the $Ce(Fe_{1-x}Al_x)_2$ system in fig.17. The diagram was constructed by plotting against composition T_c, T_f and T_o (temperature associated to be inflexion point in the jump of the temperature dependence of the magnetization).

The almost constant behaviour observed for $x \geq 0.10$ is an aditional indication of the limited solubility of the system at the iron rich side. Concerning this matter, a more detailed investigation is being performed in the composition range near the probable solubility limit; the idea is to investigate if the spin glass behaviour is or not intrinsic to the $MgCu_2$ phase.

Acknowledgements

The authors gratefully express their thanks to A.A. Gomes for valuable discussions and to A.Y.Takeuchi for his help in sample preparation.

FIGURE CAPTIONS

Fig. 1 - Variation of the lattice parameter a_o with Al composition x for $Ce(Fe_{1-x}Al_x)_2$. The dot-dashed line represents the Vegard's law for the $CeFe_2$-$CeAl_2$ system.

Fig. 2 - Magnetization vs temperature for x =0.02, 0.035 and 0.07 under 1 kOe applied field:
(●) zero field cooled sample, data taken with increasing temperature; (x) sample cooled under measuring field, data taken with decreasing temperature.

Fig. 3 - Magnetization vs temperature for x =0.02 and 0.035 under 10 kOe applied field:
(●) zero field cooled sample, data taken with increasing temperature; (▲), (x) sample cooled under measuring field, data taken with increasing and decreasing temperature respectively.

Fig. 4 - Magnetization vs field at T = 4.2K for CeF_2(•); x=0.02(0); x=0.035(+) and x=0.07(x). The dashed line in the x = 0.035 plot corresponds to the first magnetization process. The insert contains the x =0.07 data plotted in a expanded scale.

Fig. 5 - Histeresis loops for x = 0.035 at 3K with -13<H<13 kOe:
(●) zero field cooled sample; (x) 13 kOe field cooled sample. The insert shows a expanded view of the central region of both loops.

Fig. 6 - Isothermal magnetization vs field curves for x =0.02. The dashed-line plotted curves corresponds to the varia ting initial slope temperature range.

Fig. 7 - Isothermal magnetization vs field curves for x =0.035 and T≤77K.

Fig. 8 - Isothermal magnetization vs field curves for x =0.035 and T≥77K.

Fig. 9 - Isothermal magnetization vs field curves for x =0.07 with (a) 143.2>T>77K; (b) T>146.8.

Fig.10 - Isofield magnetization curves for x =0.07 (the data is the same of fig.9, replotted against temperature). Insert shows M^2 vsT dependence at temperatures near T_c for x =0.07.

Fig.11 - Iron mean magnetic moment and ferromagnetic Curie temperatures normalized to x =0 for $Y(Fe_{1-x}Al_x)_2$(x)(reference [10])and for $Ce(Fe_{1-x}Al_x)_2$ (•). (See text).

Fig.12 - Magnetization vs temperature for x =0.15 under 1 kOe applied field (zero field cooled sample).

Fig.13 - Susceptibility (M_g/H) vs temperature for x =0.15 under 0.3 and 1.0 kOe: (▲) and (□) field cooled sample, (Δ) and (■) ZFCS.

Fig.14 - Isothermal magnetization vs field curves (field up to 150 kOe) for x =0.15.

Fig.15 - AC susceptibility for x =0.20: (x) 155 Hz; (•) 1550 Hz.

Fig.16 - Histeresis loops for x=0.15 at 4.2K:(•) zero field cooled sample; (x) sample cooled in 13 kOe field.

Fig.17 - Proposed magnetic phase diagram: (•) T_c; (x) T_o; (Δ) T_f; P-paramagnetic; C- canted spin ;SG - spin glass; F-Ferromagnetic.

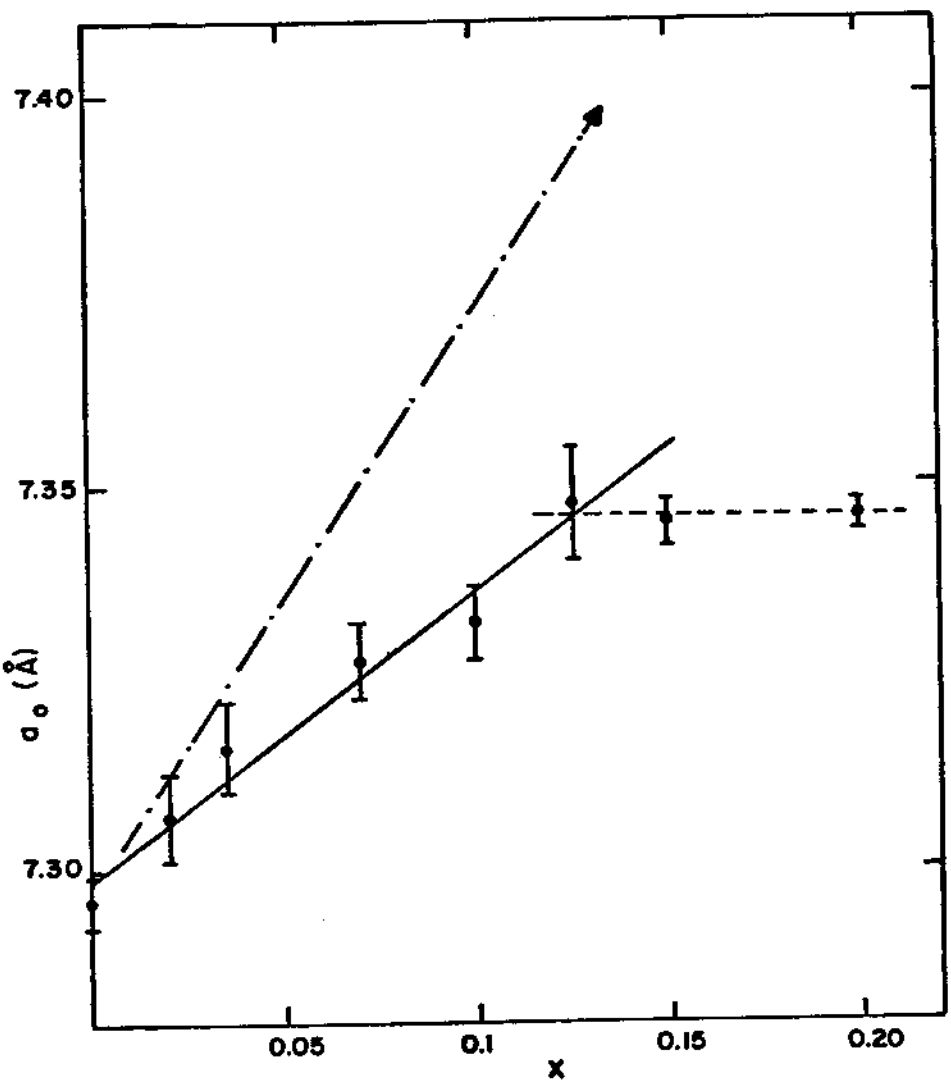

Fig. 1

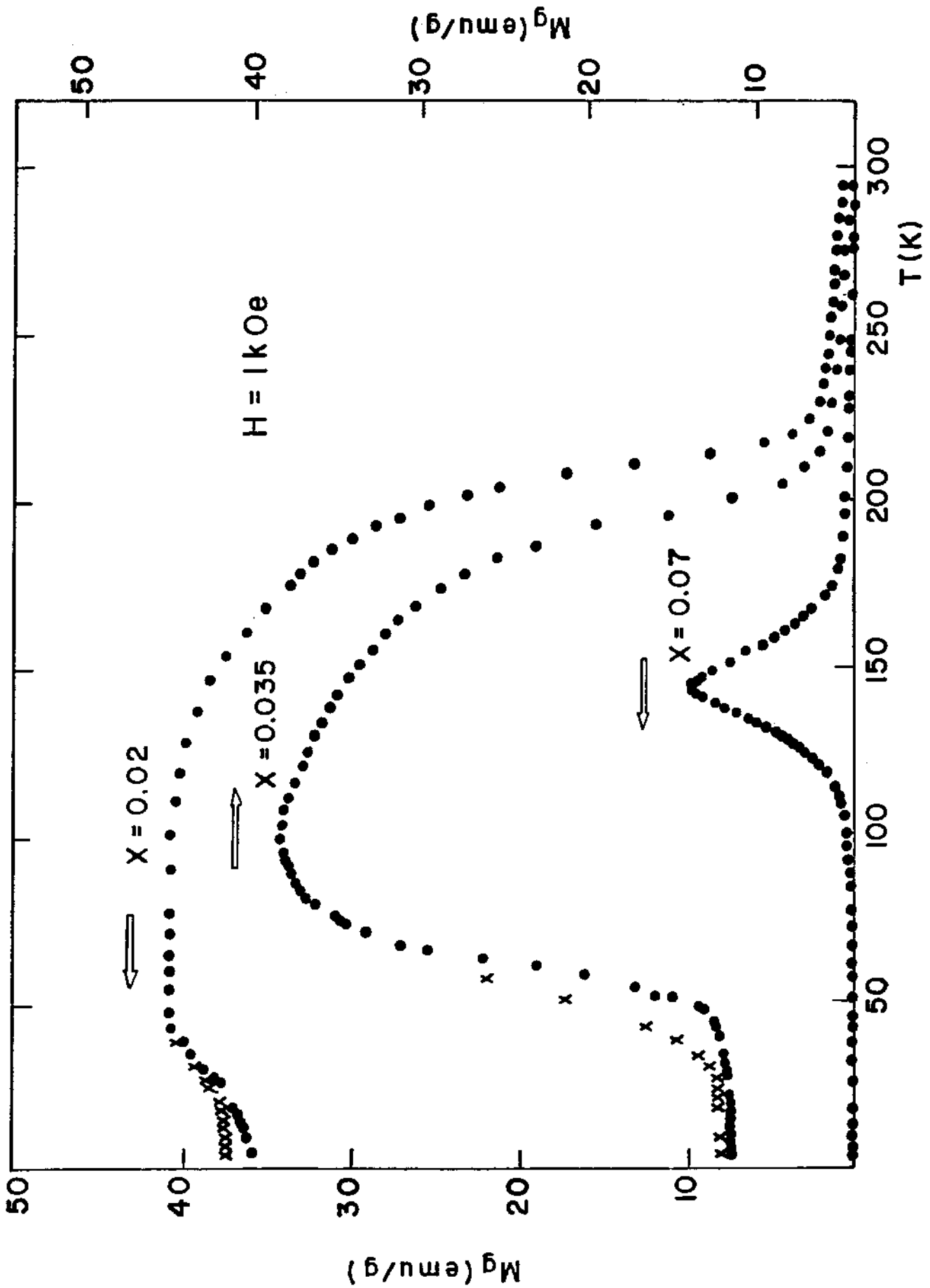
H = 1 kOe
X = 0.02
X = 0.035
X = 0.07
M_g (emu/g)
T (K)
50
40
30
20
10
50
100
150
200
250
300

Fig. 2

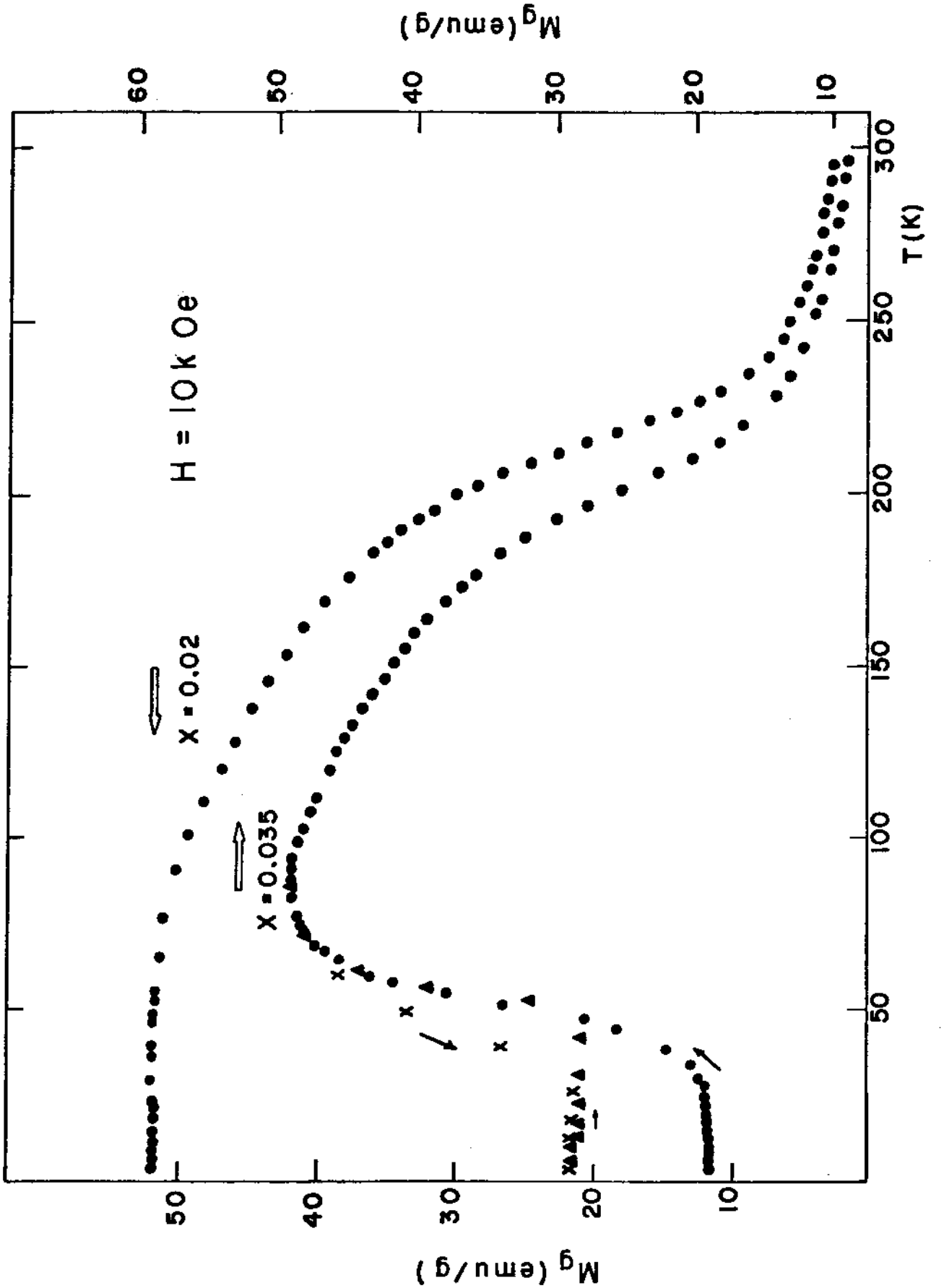
M_g (emu/g)
60
50
40
30
20
10
300
250
200
150
100
50
T(K)
H = 10 k Oe
X = 0.02
X = 0.035
M_g (emu/g)
50
40
30
20
10

Fig. 3

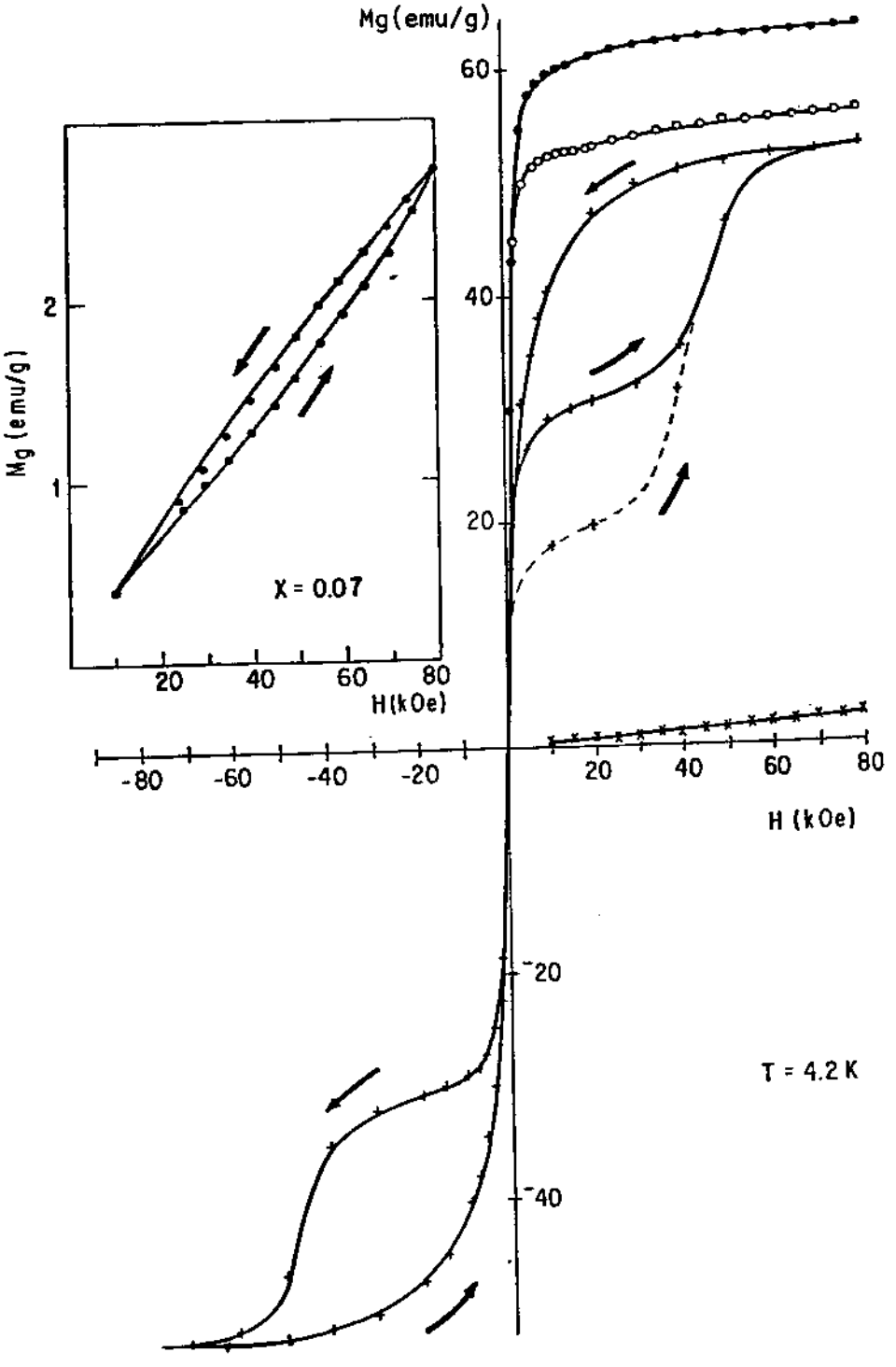
Mg(emu/g)
60
40
20
-20
-40
-80
-60
-40
-20
20
40
60
80
H (kOe)
T = 4.2 K
Mg (emu/g)
2
1
X = 0.07
20
40
60
80
H(kOe)

Fig. 4

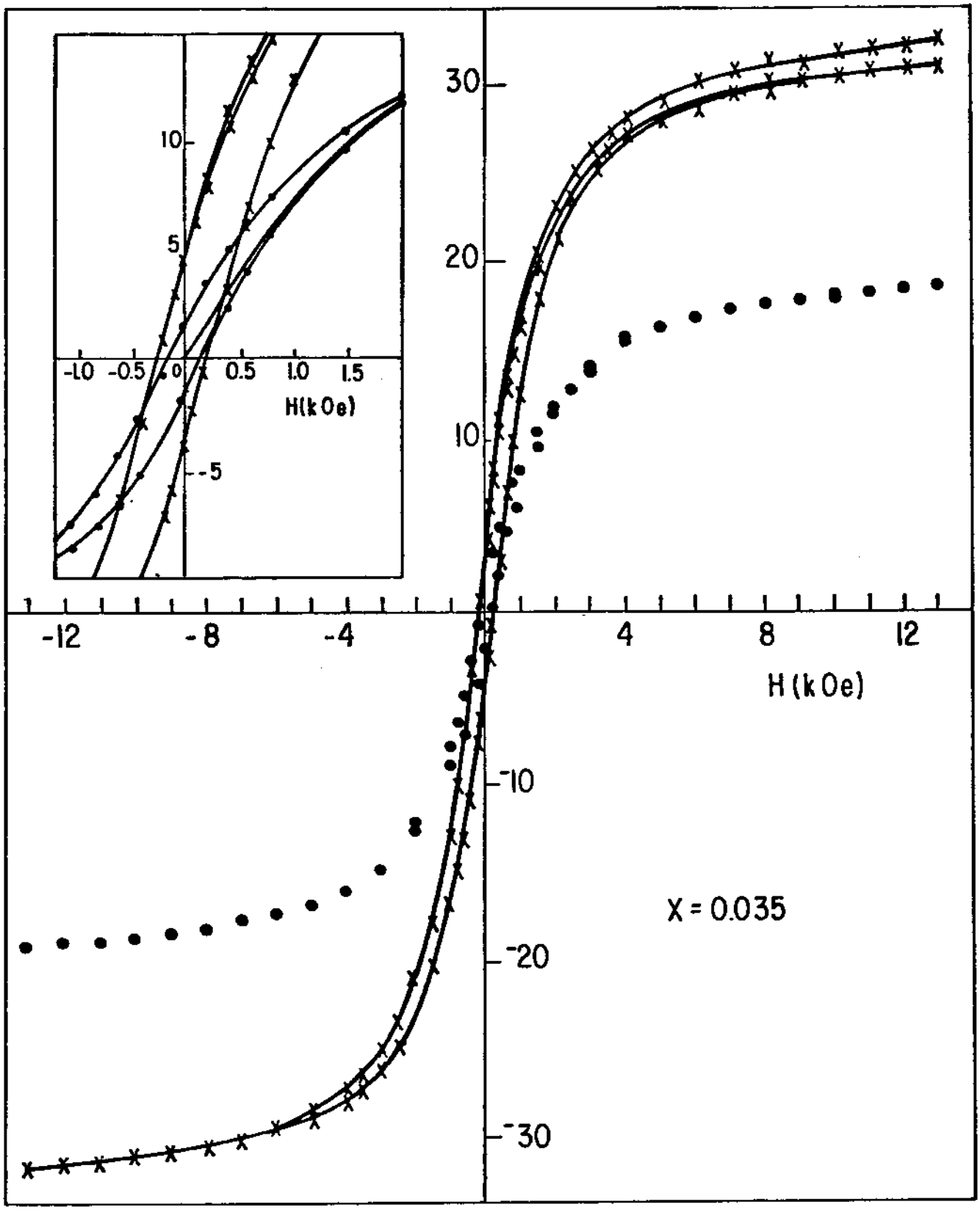

Fig. 5

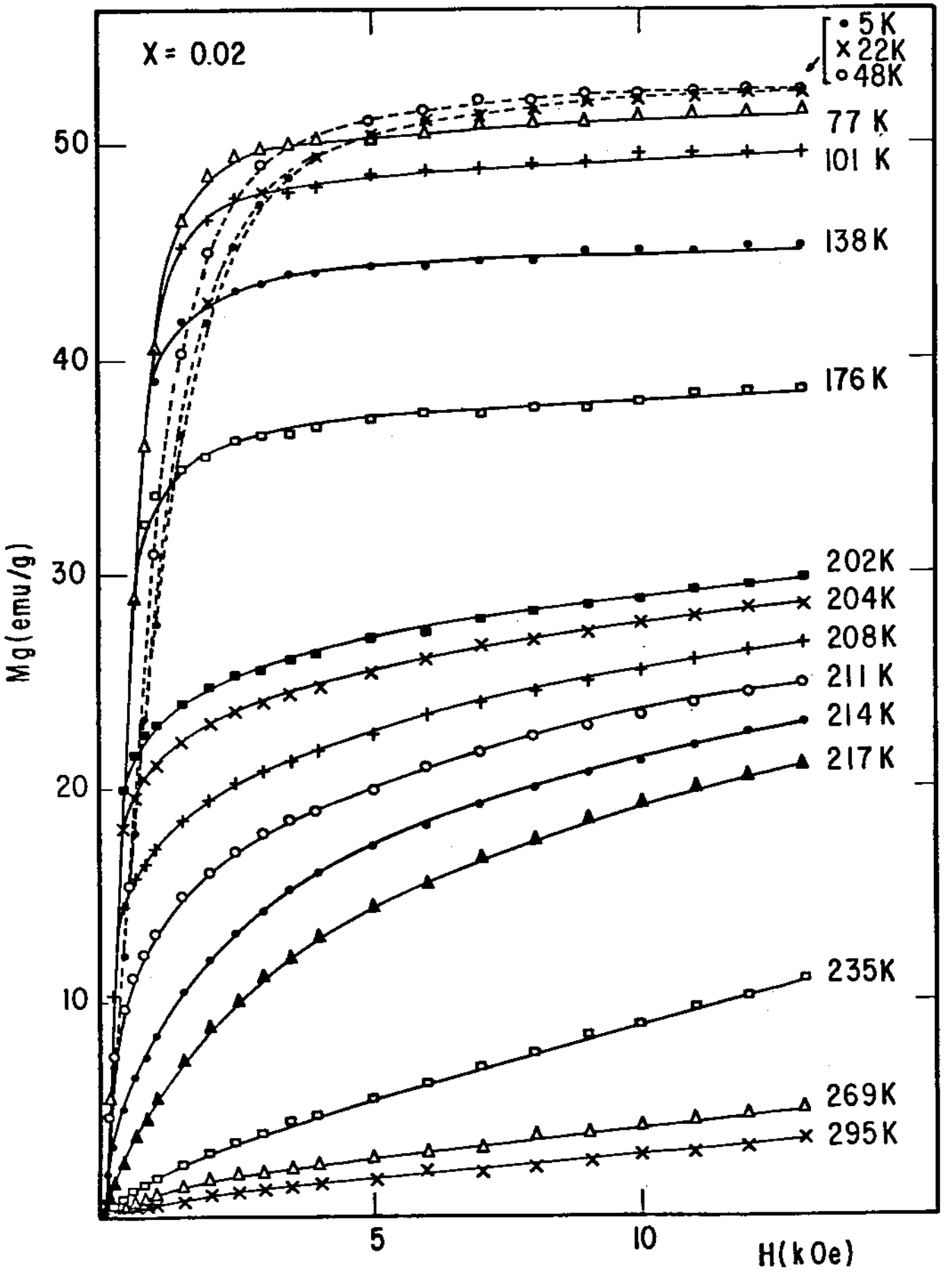
X = 0.02
• 5K
× 22K
○ 48K
77 K
101 K
138 K
176 K
202K
204K
208K
211 K
214 K
217 K
235K
269K
295K
Mg(emu/g)
H(kOe)
10
20
30
40
50
5
10

Fig. 6

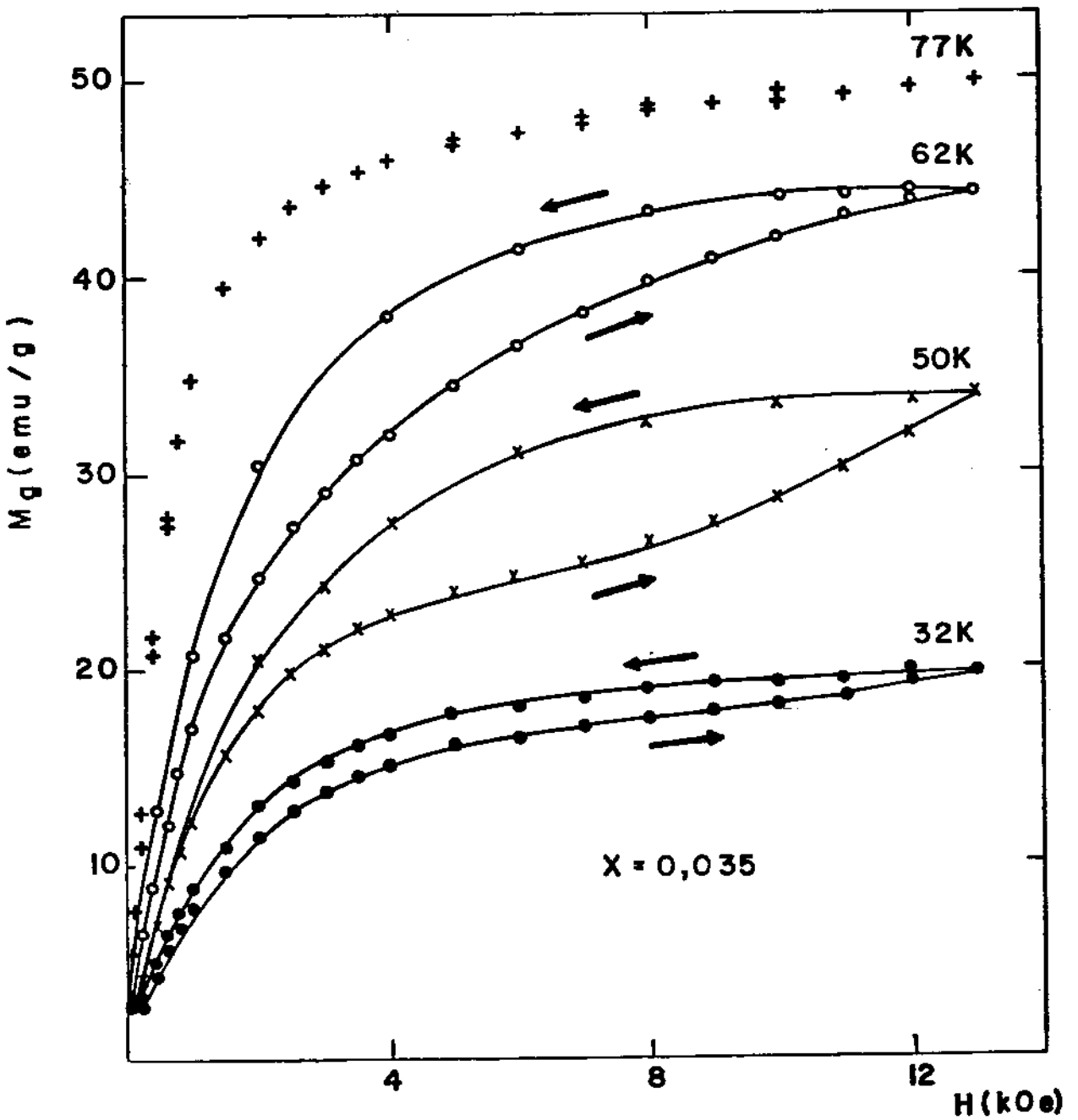

Fig. 7

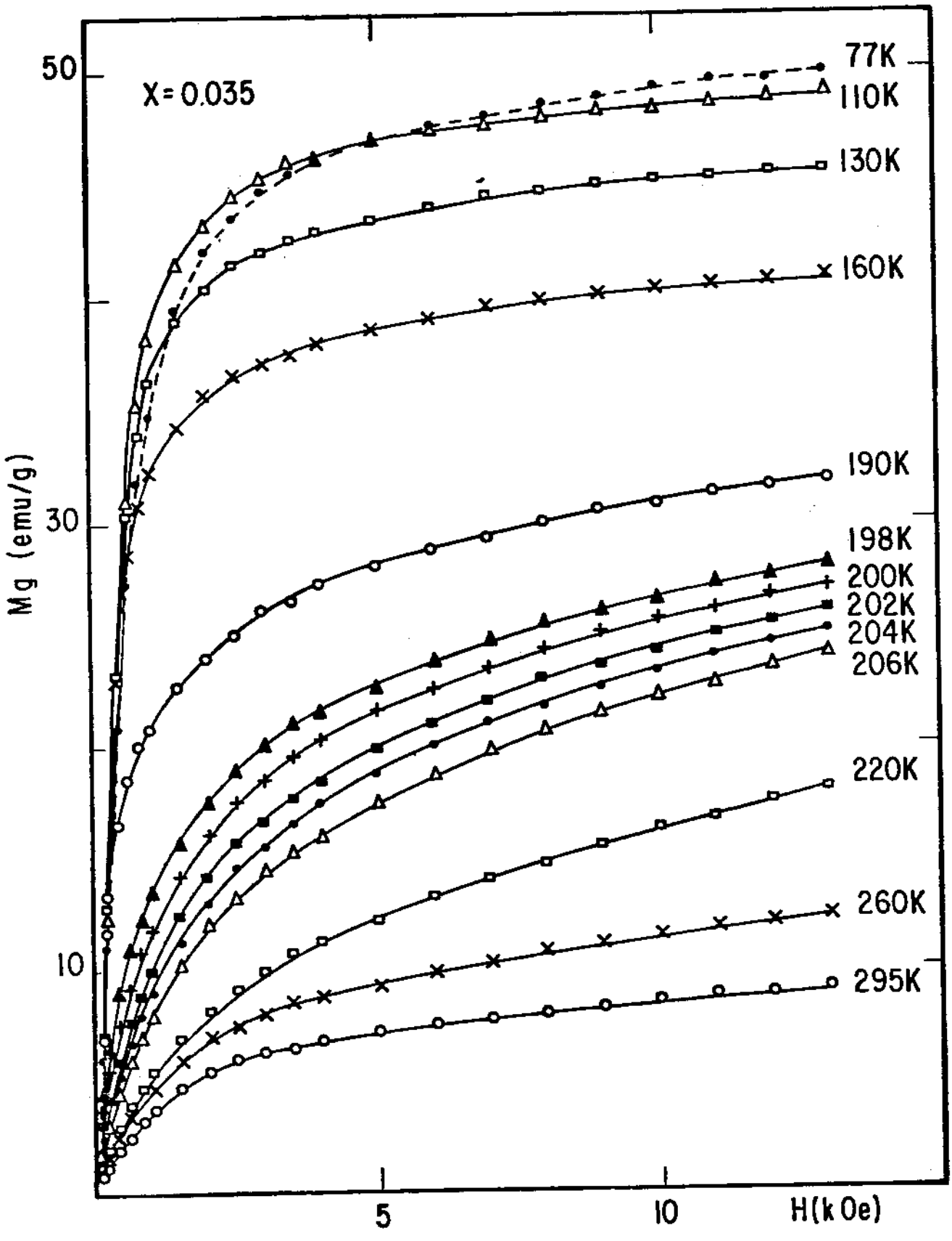
X= 0.035
77K
110K
130K
160K
190K
198K
200K
202K
204K
206K
220K
260K
295K
Mg (emu/g)
50
30
10
5
10
H(kOe)

Fig. 8

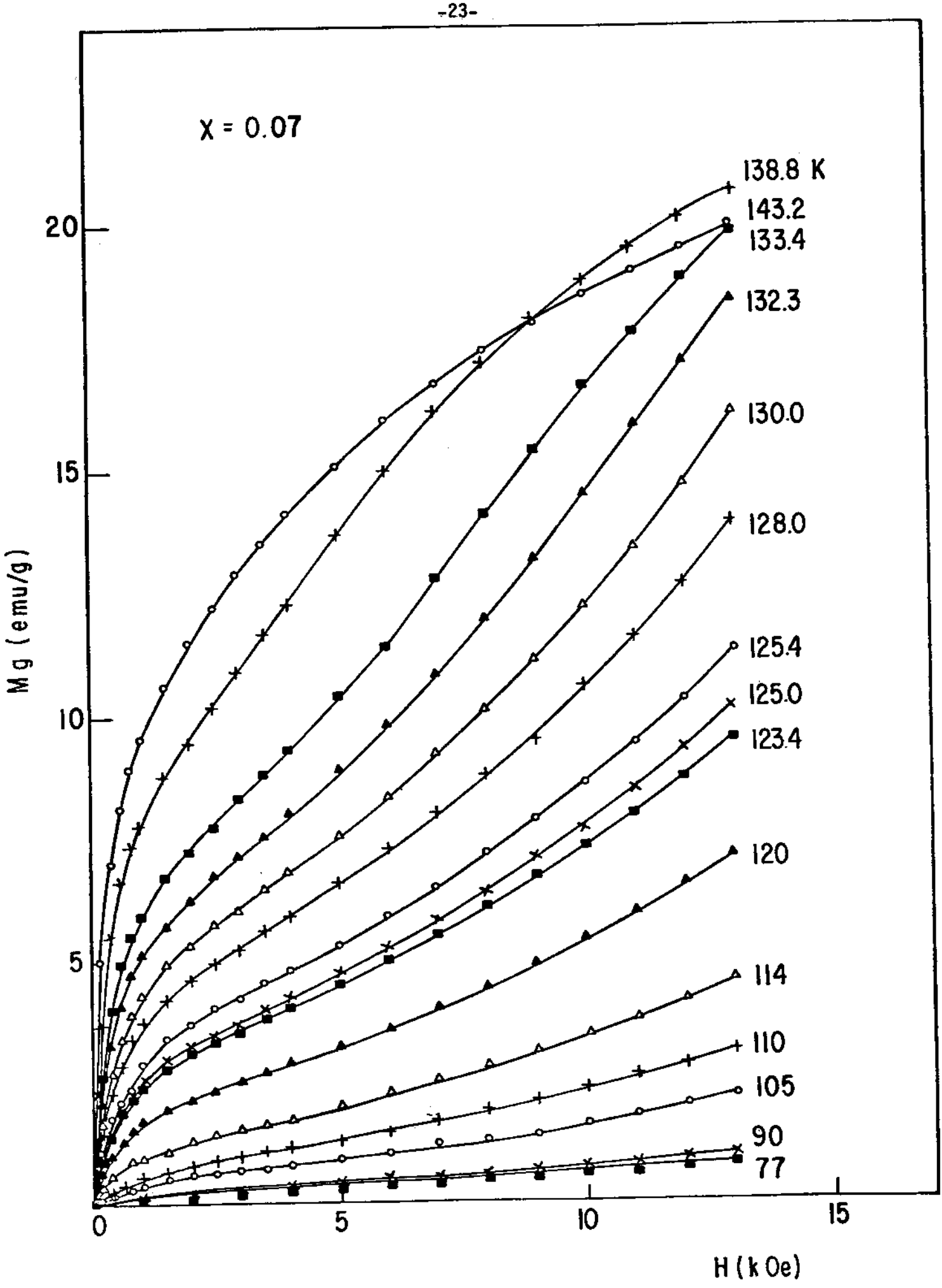
X = 0.07
138.8 K
143.2
133.4
132.3
130.0
128.0
125.4
125.0
123.4
120
114
110
105
90
77
Mg (emu/g)
H (k Oe)
0
5
10
15
20

Fig. 9a

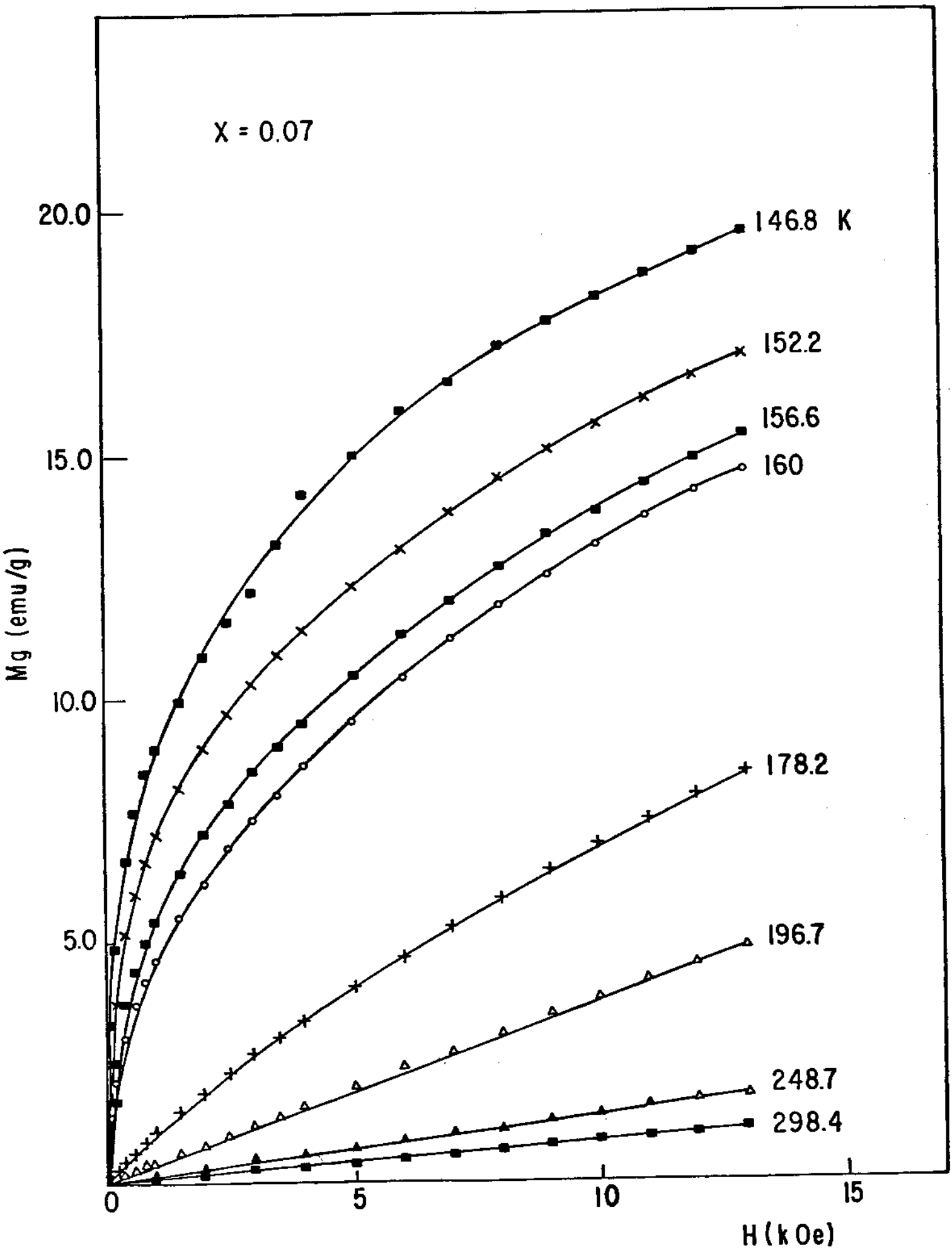
X = 0.07
20.0
15.0
10.0
5.0
Mg (emu/g)
146.8 K
152.2
156.6
160
178.2
196.7
248.7
298.4
0
5
10
15
H (k Oe)

Fig. 9b

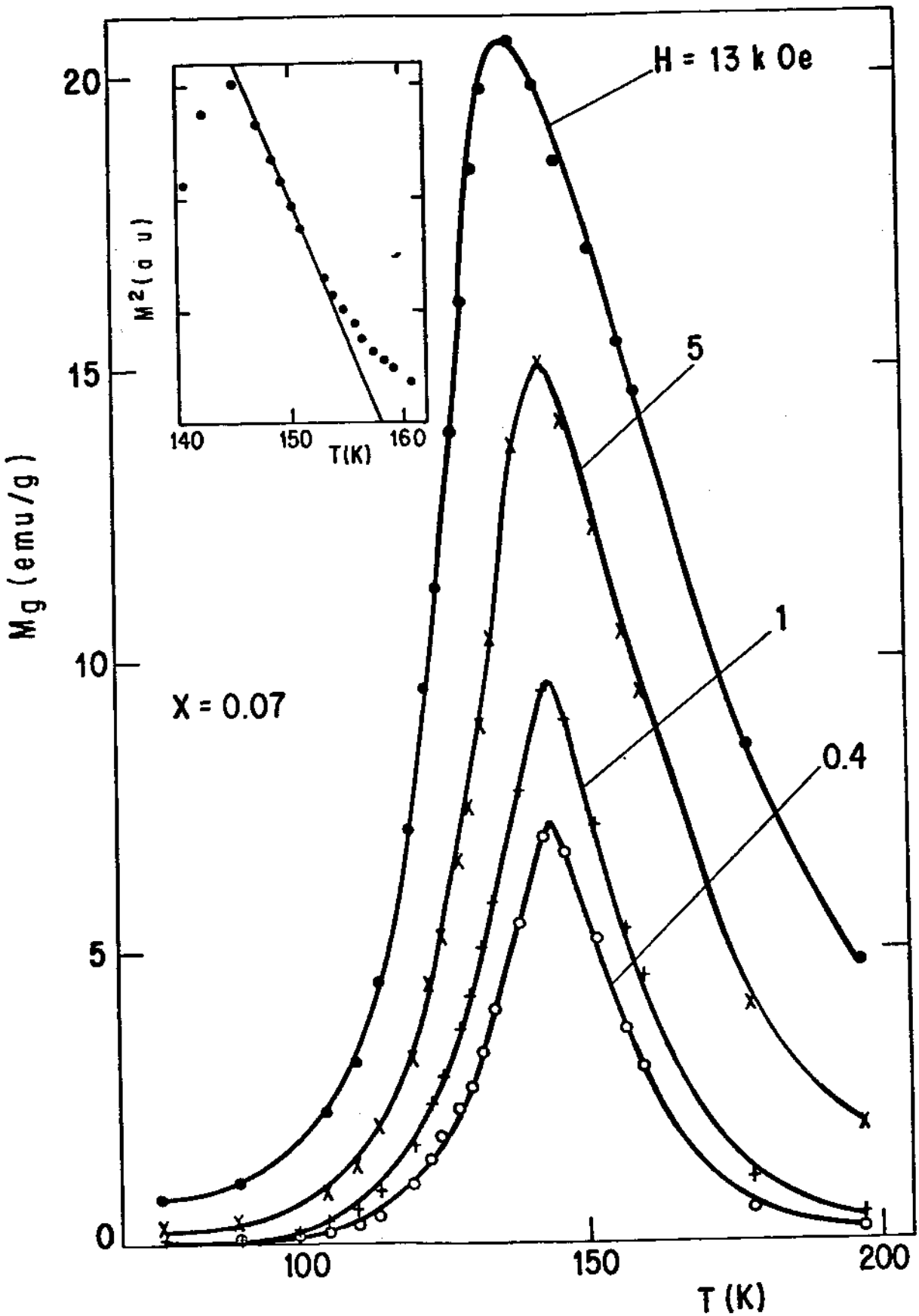
H = 13 k Oe
5
1
0.4
X = 0.07
Mg (emu/g)
T (K)
M²(a u)
T(K)
20
15
10
5
0
100
150
200
140
150
160

Fig. 10

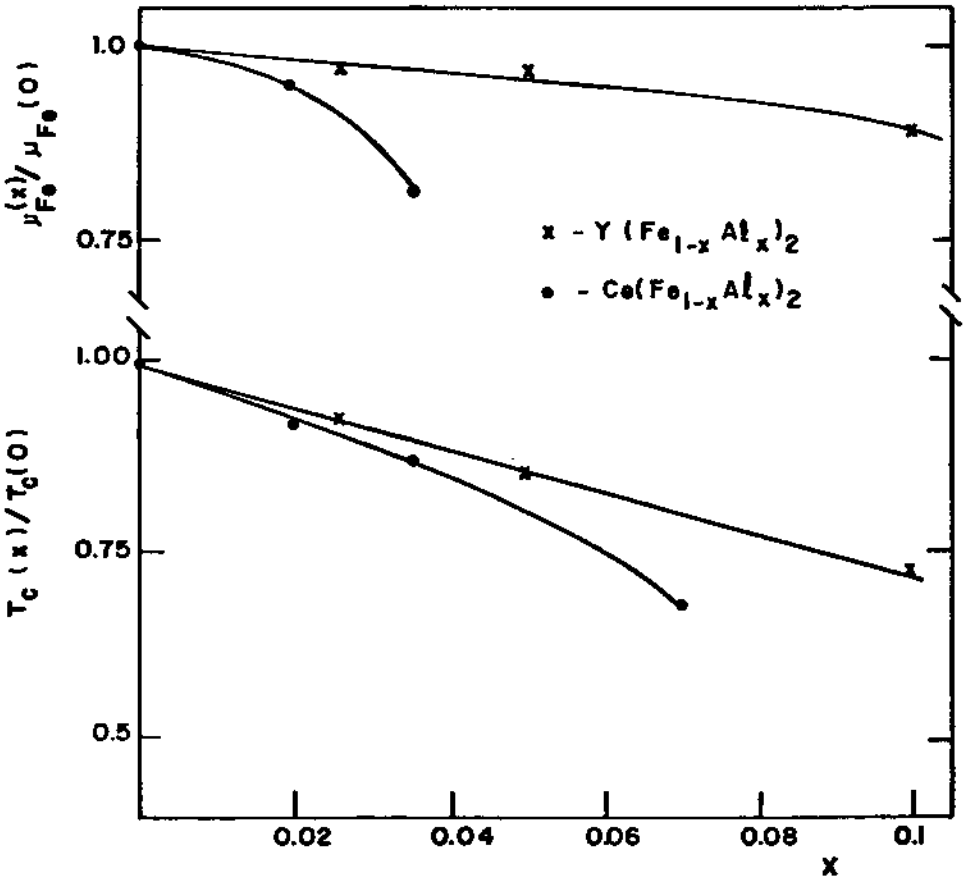
1.0
0.75
$\mu_{Fe}^{(x)}/\mu_{Fe}(0)$
x - Y $(Fe_{1-x}Al_x)_2$
• - Ce$(Fe_{1-x}Al_x)_2$
1.00
0.75
0.5
$T_c(x)/T_c(0)$
0.02
0.04
0.06
0.08
0.1
x

Fig. 11

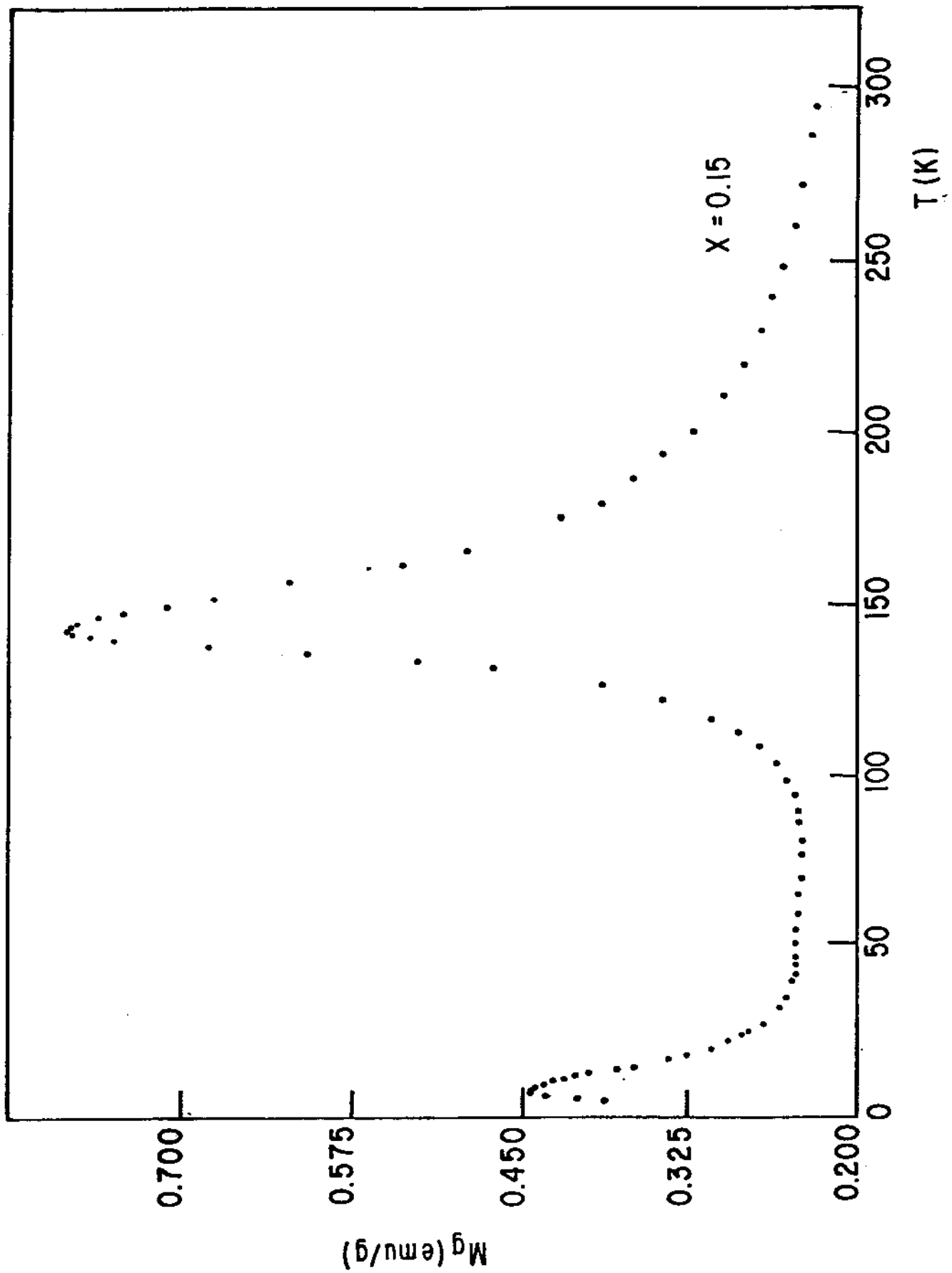
X = 0.15
T (K)
0
50
100
150
200
250
300
0.700
0.575
0.450
0.325
0.200
M_g (emu/g)

Fig. 12

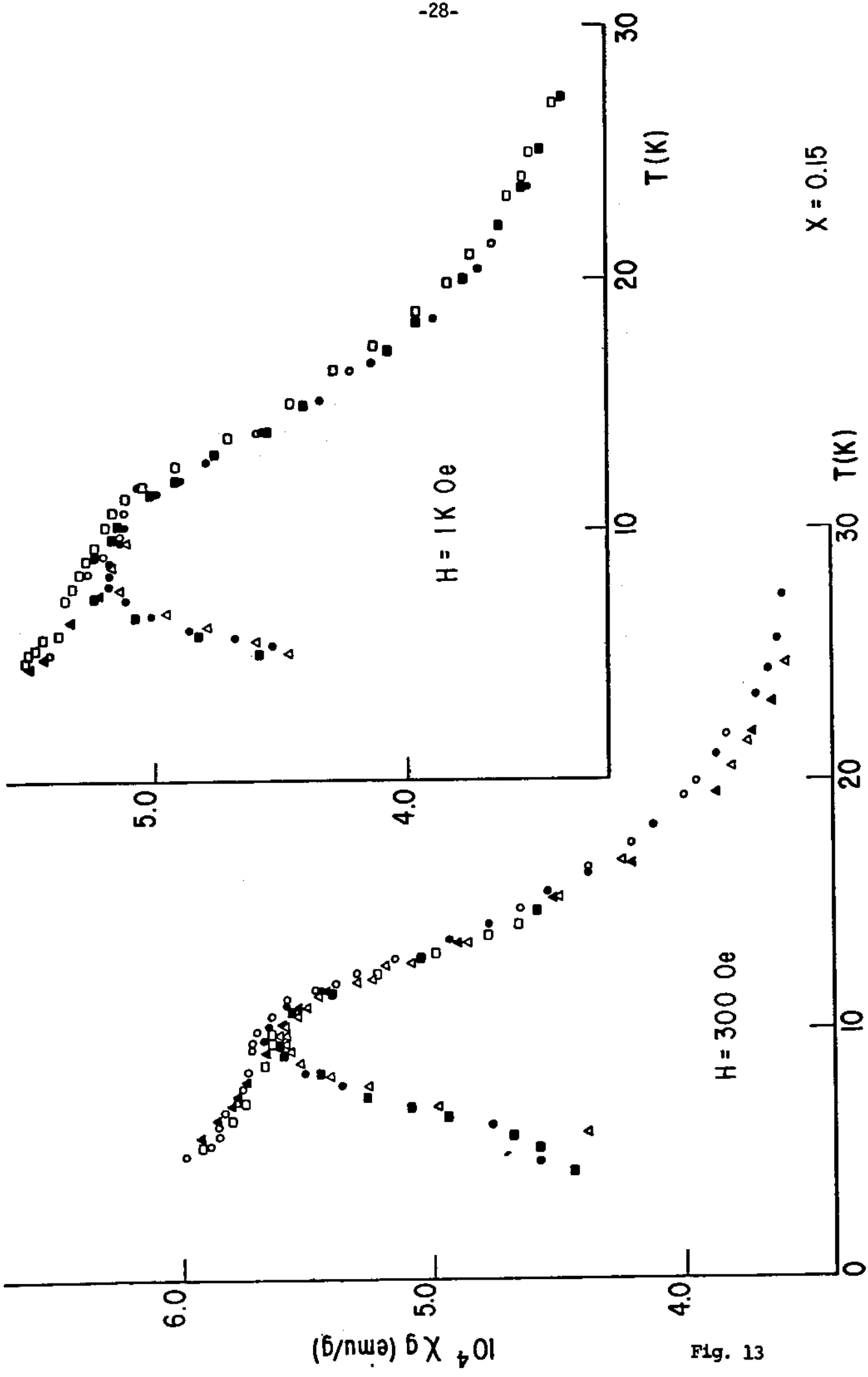
X = 0.15
H = 1 K Oe
H = 300 Oe
T(K)
T(K)
$10^4 \chi_g$ (emu/g)
6.0
5.0
4.0
5.0
4.0
0
10
20
30
10
20
30

Fig. 13

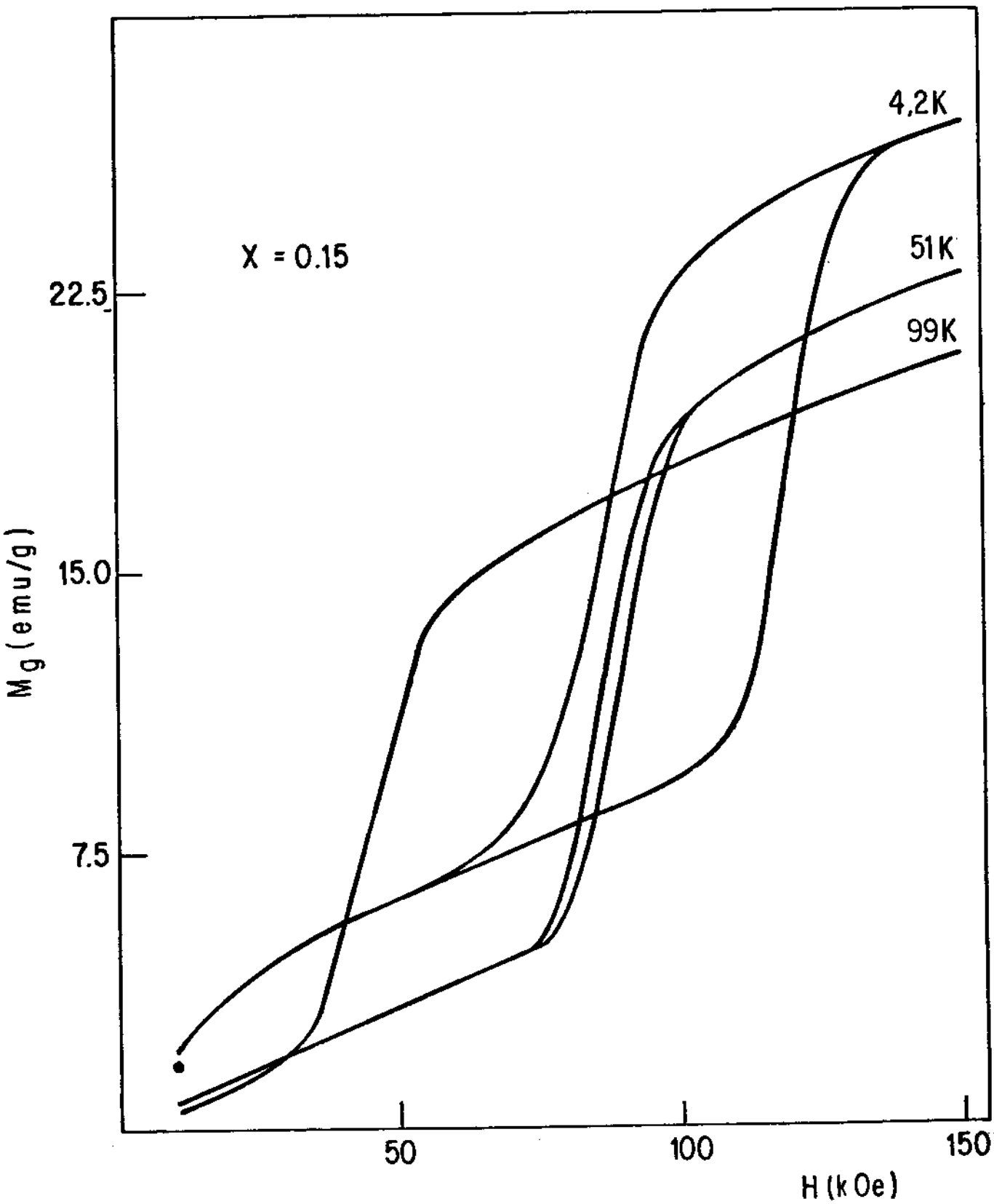

Fig. 14

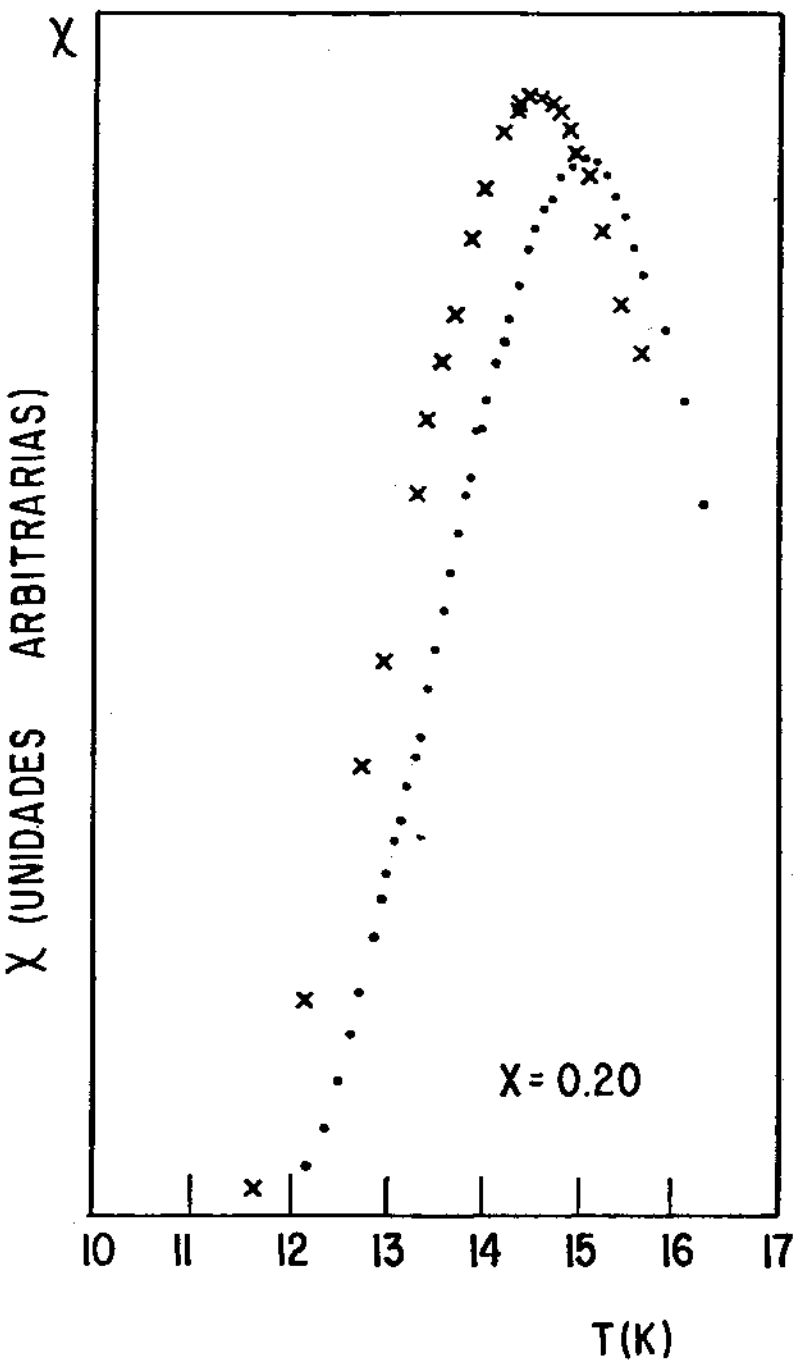

Fig. 15

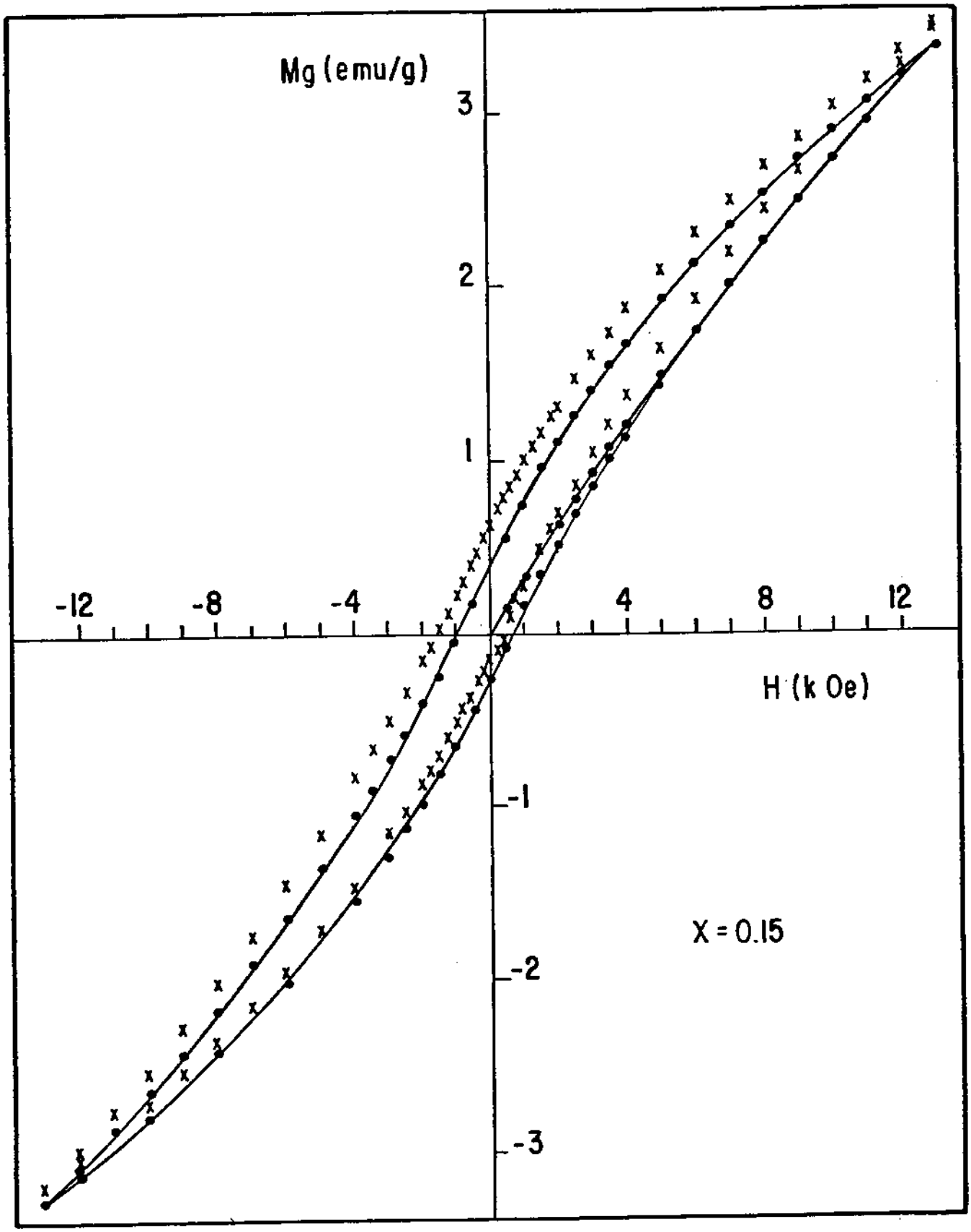

Fig. 16

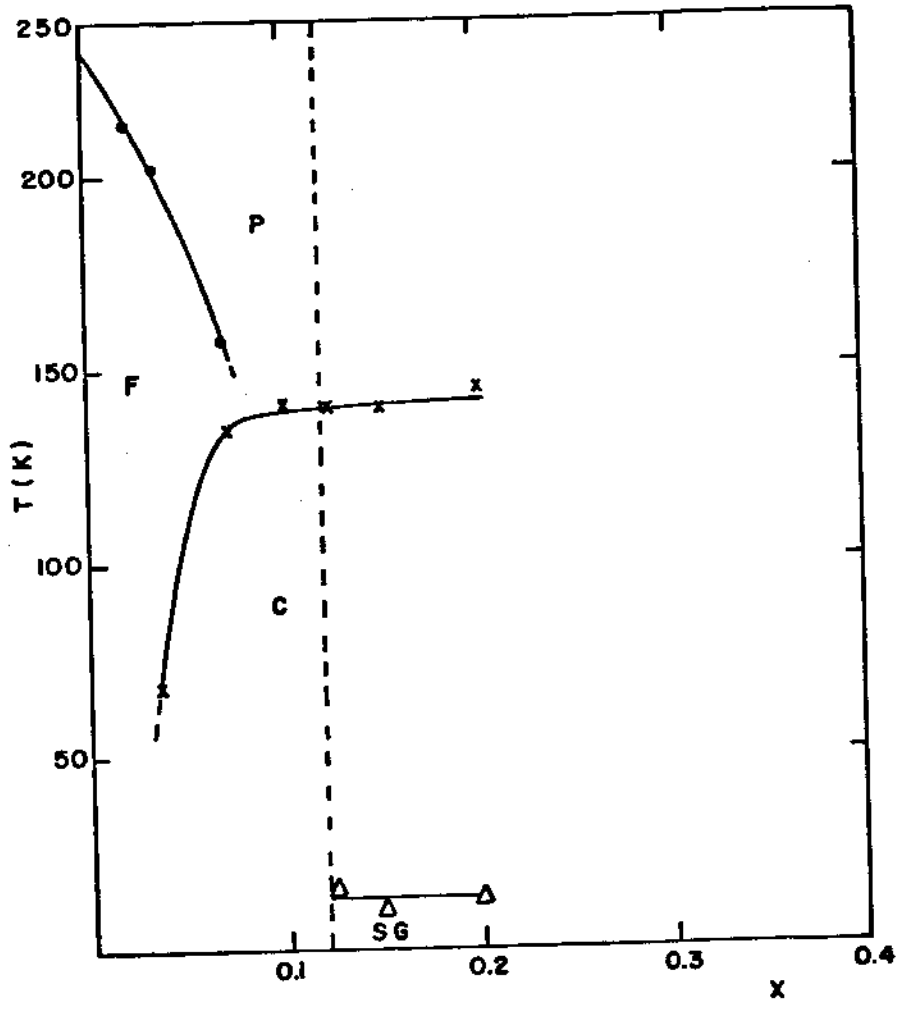

Fig. 17

TABLE 1

X	T_c(K)	$\mu_{Fe}(\mu_B/Fe)$
0.0	232.0	1.33
0.02	213.8	1.26
0.035	201.8	1.08
0.07	158.0	-

REFERENCIAS

[1] W.Steiner, J.Mag.Mag. Mat. 14 (1979) 47

[2] G. Hilscher, J.Mag.Mag. Mat. 27 (1982) 1

[3] S.G. Sankar and W.E. Wallace, Magnetism Letters 1 (1976) 3

[4] V. Atzmony and M.P. Dariel, Phys. Rev. B10 (1974) 2060

[5] A.E. Dwight, C.W. Kimball, R.S. Preston, S.P. Taneja and L. Weber, J.Less Common Metals 40 (1975) 285

[6] S.F. da Cunha, D.F. Franceschini, S.Senoussi and A.Y. Takeuchi J.Phys. F:Metal Phys. 12 (1982) 3083

[7] A.Y. Takeuchi and S.F. da Cunha, J.Mag. Mat. 30 (1982)135

[8] A.Y. Takeuchi and S.F. da Cunha, J.Mag. Mat., in press

[9] G.Hilscher, R. Grossinger, V.Sechovsky and P.Nozar, J.Phys. F.:Met. Phys. 12 (1982) 1209

[10] M.J.Besnus, P.Bauer and J.M.Gēnin, J.Phys. F.: Met. Phys. 8 (1978) 191.

[11] F.Kissel and W.E. Wallace, J.Less-Comm. Metals 11 (1966) 417

[12] A. Fote, E.Domb, S.Bakanowski, T.Mihalisin and J.Crow, Phys. Letters 34A (1971) 352

[13] J.Howard, P.M.Bisch and A.A. Gomes, J.Phys. F.13 (1983)2629 and J.Phys. F.14 (1984) 2729